

# Middle Pleistocene (MIS 14) environmental conditions in the central Mediterranean derived from terrestrial molluscs and carbonate stable isotopes from Sulmona Basin (Italy)

Giovanni Zanchetta<sup>1\*</sup>, Monica Bini<sup>1</sup>, Biagio Giaccio<sup>2</sup>, Giuseppe Manganelli<sup>3</sup>, Andrea Benocci<sup>4</sup>, Eleonora Regattieri<sup>5,6</sup>, Andre C. Colonese<sup>7</sup>, Chiara Boschi<sup>6</sup>, Cristian Biagioni<sup>1</sup>

<sup>1</sup>Dipartimento di Scienze della Terra, University of Pisa, Via S. Maria 53, 56126 Pisa, Italy

<sup>2</sup>Istituto di Geologia Ambientale e Geoingegneria, IGAG-CNR, Via Salaria km. 29.4, 00015 Monterotondo Rome, Italy

<sup>3</sup>Dipartimento di Scienze Fisiche, della Terra e dell'Ambiente, Via Mattioli 4 53100 Siena, Italy

<sup>4</sup>Museo di Storia Naturale dell'Accademia dei Fisiocritici, Piazzetta Gigli 2 53100 Siena, Italy

<sup>5</sup>Institute of Geology and Mineralogy, University of Cologne, Zùlpicher Str. 49a, 50674 Cologne, Germany

<sup>6</sup>Istituto di Geoscienze e Georisorse, IGG-CNR, Via Moruzzi 1, 56126 Pisa, Italy

<sup>7</sup>Department of Archaeology, BioArCh, University of York, Wentworth Way, York YO10 5DD England (UK).

\*Corresponding author: zanchetta@dst.unipi.it

## Abstract

A paleosol from the Middle Pleistocene lacustrine-fluvial succession of Sulmona Basin, central Italy, was analysed for the land snail shell content, and the stable isotope composition of the shells and associated pedogenic carbonates. The paleosol – known as Fiorata Paleosol – is covered by a thick tephra layer dated to ca. 527 ka allowing the pedogenetic horizons to be correlated to the marine isotope stage (MIS) 14-early MIS 13 interval. The terrestrial mollusc assemblage contained few individuals and was characterized by a low number of species which predominantly indicate open and dry habitats, thus suggesting that Fiorata Paleosol likely developed during glacial conditions of the MIS 14. The  $\delta^{13}\text{C}$  values of pedogenic carbonates and terrestrial shells indicate prevailing  $\text{C}_3$ -type vegetation, probably marked by some degree of water stress. Calculation of the  $\delta^{18}\text{O}$  precipitation values, derived from pedogenic carbonates and shell  $\delta^{18}\text{O}$  values, indicate that the average temperature was 3-5°C lower than present day. This study highlights how paleosols, despite offering only snapshots of past climate and environments, provide valuable complementary information to paleoclimatic data obtained in the adjacent lacustrine intervals, specifically for the Sulmona successions.

*Keywords:* tephra layers; paleosol;  $\text{C}_3$ -type vegetation; Glacial

## 34 **1. Introduction**

35  
36 Stable isotopes (e.g.  $^{13}\text{C}/^{12}\text{C}$  and  $^{18}\text{O}/^{16}\text{O}$ ) of pedogenetic carbonate (Cerling, 1984; Jiamao et  
37 al., 1991; Cerling and Quade, 1993; Zanchetta et al., 2000) and terrestrial mollusc shells (e.g.  
38 Balakrishnan et al., 2005a; Colonese et al., 2007, 2010; Murelaga et al., 2012; Yanes et al., 2011;  
39 Paul and Mauldin, 2013. Prendergast et al., 2016) can provide valuable snapshots of past  
40 environments, notably vegetation type (e.g.  $\text{C}_3/\text{C}_4$  ratios, Cerling and Quade, 1993; Zanchetta et al.,  
41 2006), and past precipitation regimes (Lecolle, 1985; Zanchetta et al., 2005; Baldini et al., 2007;  
42 Hassan, 2015; Prendergast et al., 2017). Despite representing important sources of complementary  
43 paleoclimatic information, combined studies on molluscan assemblages and stable isotope analysis  
44 of pedogenic and shell carbonates are scarce (e.g. Zanchetta et al., 2006; Leone et al., 2000;  
45 Balakrishnan et al., 2005a).

46 Furthermore, whilst the Holocene and Late Pleistocene terrestrial mollusc assemblages of the  
47 Mediterranean and continental Europe are rather well known and studied (e.g. Kerney, 1976; Esu,  
48 1981; Rousseau et al., 1992; Limondin-Lozouet and Antoine, 2006; Limondin-Lozouet et al.,  
49 2017), the Middle Pleistocene successions are relatively rare and often chronologically poorly  
50 constrained (e.g. Rousseau and Keen, 1989; Limondin-Lozouet and Preece, 2004). In particular,  
51 terrestrial molluscs of glacial periods have been previously described for the Last Glacial in Europe  
52 from loess successions (e.g. Ložek, 1990; Rousseau et al., 1990; Moine, 2008), but for older glacial  
53 intervals our knowledge is essentially fragmentary and incomplete.

54 In this paper we discuss the terrestrial mollusc assemblages and stable isotope geochemistry  
55 ( $^{13}\text{C}/^{12}\text{C}$  and  $^{18}\text{O}/^{16}\text{O}$  ratios) of their shells and of associated pedogenic carbonates from a Middle  
56 Pleistocene paleosol developed within a fluvial to lacustrine succession at the Sulmona Basin  
57 (Abruzzo, central Italy, Fig. 1). The lacustrine successions have been extensively investigated and  
58 yielded important insights into past climate conditions in the Central Mediterranean between the  
59 late Early to the Late Pleistocene (Giaccio et al., 2015; Regattieri et al., 2015, 2016, 2017).  
60 However, stratigraphic evidence indicates that the lake level was substantially lower during some  
61 glacial intervals, and subaerial processes (fluvial-colluvial deposition, erosion and/or pedogenesis)  
62 dominated with respect to the lacustrine sedimentation (Giaccio et al., 2015; Regattieri et al.,  
63 2015,2016,2017). For such a sub-aerial stratigraphic intervals, pedogenic horizons thus represent  
64 the unique alternative sources of information to complement paleoclimatic inferences derived from  
65 lacustrine sediments at Sulmona Basin.

## 66 **2. Site description**

68 The Sulmona Basin (Fig. 1) is an intramontane depression formed during the Plio-Quaternary  
69 extensional tectonic phase that dissected the earlier orogenic, fold-and-thrust-belt system of the  
70 Apennine chain (e.g. Patacca and Scandone, 2007). The progressive formation of the basin was  
71 driven by the Sulmona or Morrone NW–SE-trending fault system (Galli et al., 2015),  
72 accommodating the volume for the accumulation of a thick Quaternary succession (e.g. Cavinato  
73 and Miccadei, 2000; Giaccio et al., 2012, 2013b). The Pleistocene succession is subdivided in three  
74 main unconformity-bounded alluvial–fluvial–lacustrine units; SUL-6, SUL-5 and SUL 4-3 (Figs. 1,  
75 2). Each unit is constrained by tephrochronology, including direct  $^{40}\text{Ar}/^{39}\text{Ar}$  dating of the tephra  
76 layers, and magnetostratigraphy (Giaccio et al., 2012, 2013a, 2013b; Sagnotti et al., 2014; Giaccio  
77 et al., 2015; Regattieri et al., 2015, 2016, 2017; Figs. 1, 2). The paleosol discussed in this paper  
78 (hereafter referred to as Fiorata Paleosol, from the toponymal of the type section; Fig. 1) occurs  
79 immediately above the lower boundary of SUL-5 and formed on the gravel-sand succession which  
80 fills a deep fluvial incision carved into the underlying SUL-6 unit (Figs. 1, 2). The pedogenic  
81 horizon consists of ca. 40-50 cm of gray-dark-grayish brown (10YR 4/2 -4/1 dark) silty to coarse  
82 massive sands A horizon (Fig. 2). The lower boundary fades in the lower fluvial interval through a  
83 massive, bioturbated C horizon. Thin root traces are preserved in the upper horizon, sometimes with  
84 walls impregnated by oxides. Small carbonate concretions are also visible. The Fiorata Paleosol is  
85 directly capped by a syn-depositionally reworked tephra layer (SUL5b-12 in Fig. 2) up to 0.5 m-  
86 thick of fine lapilli to coarse ash made up of green, porphyritic and finely grained micro-scoria (Fig.  
87 2). Some fine volcanic ash fills small burrows and/or root traces within the upper soil horizon.  
88 Based on its peculiar foiditic composition of the glass from the layer and its stratigraphic order with  
89 respect other marker tephras, SUL5b-12 (Fig. 2) was correlated to the Tufo di Bagni Albule  
90 eruption by Giaccio et al. (2013a), from Colli Albani volcanic district dated by  $^{40}\text{Ar}/^{39}\text{Ar}$  to  $527\pm 2$   
91 ka (Marra et al., 2009).

92 A detailed description of climatic and hydrological settings of the Sulmona Basin can be found  
93 in Regattieri et al. (2015, 2016, 2017) and is only briefly summarized here. The Sulmona  
94 meteorological station (ca. 400 m a.s.l.) records a mean annual temperature of  $13.7^{\circ}\text{C}$ , and an  
95 average rainfall of ca. 700 mm. Precipitation is strongly influenced by local topography and by the  
96 rising margin of the tectonic basin, reaching values of about 1200 mm at mountain summits. Winter  
97 precipitation is largely regulated by conditions in the North Atlantic and the North Atlantic  
98 Oscillation (López-Moreno et al., 2011). The meteoric precipitation at the L'Aquila Station (ca. 710  
99 m a.s.l., ca. 60 km NW from Sulmona) has an average  $\delta^{18}\text{O}$  value of  $-7.13\text{‰}$  (Longinelli and  
100 Selmo, 2003). The measured isotopic altitudinal gradient ( $\delta^{18}\text{O}/100\text{ m}$ ) ranged from  $-0.23$  to  $-0.13$   
101  $\text{‰}/100\text{ m}$  (e.g. Barbieri et al., 2005; Giustini et al., 2016).

102  
103

### 3. Material and Methods

104 Two distinct sedimentary samples (SUL-16/01 and SUL-16/02) of ca. 10 kg each were collected  
105 from two different localities along the section exposing the Fiorata Paleosol at a distance of ca. 100  
106 m, and ca. 10-15 cm below the paleosol top (Figs. 1 and 2). At these two sampling sites no  
107 differences in the paleosol profile were observed. Samples were first dried at room temperature for  
108 several days and then disaggregated using a very dilute solution of H<sub>2</sub>O<sub>2</sub> (ca. 5%) and deionized  
109 water. The material was gently washed and sieved using 2000, 1000, 500 and 250 µm mesh screens,  
110 and all the identifiable shells and fragments were picked out under a binocular microscope and  
111 counted using the convention of Sparks (1961), where every gastropod apex is recorded to give a  
112 minimum number of individuals. The higher systematics followed Bouchet and Rocroi (2005)  
113 except for the helicoideans, for which the revision by Razkin et al. (2015) was adopted. The  
114 taxonomy and nomenclature of the extant species followed Welter-Schultes (2012).

115 During mollusc picking, small carbonate concretions (mm-sized) were also found and selected  
116 for isotopic analysis. Whole, well preserved shells of a helicelline geomitrid species and small  
117 carbonate concretions were soaked in a solution of distilled water and H<sub>2</sub>O<sub>2</sub> (30%) and sonicated to  
118 remove contaminants. Samples were then dried, powdered and homogenized for stable isotope  
119 analyses. Samples of helicelline shells were also checked for mineralogical composition using X-  
120 ray diffraction (XRD). XRD was performed using a Bruker D2 Phaser diffractometer (30 kV, 10  
121 mA) operating in Bragg-Brentano geometry (Θ-Θ scan mode) and equipped with a 1-dimensional  
122 Lynxeye detector. Ni-filtered Cu Kα radiation was used. Data were collected in the scan range 4-  
123 65° in 2Θ, with scan step of 0.02° and counting time of 0.1 s/step. Data were processed through the  
124 software Diffrac.Eva (Bruker AXS Inc., 2015). Similarly, carbonate concretions were checked for  
125 mineralogical composition using XRD and inspected using a SEM-EDS for microscopic  
126 observation (Philips SEM 515 coupled with an EDS EDAX-DX micro-analyser).

127 Stable oxygen (δ<sup>18</sup>O) and carbon (δ<sup>13</sup>C) isotope ratios were determined using a Gas Bench II  
128 (Thermo Scientific) coupled with an IRMS Delta XP (Finnigan Mat) at the IGG-CNR in Pisa  
129 (Italy). Each carbonate sample of ca. 0.15 mg was dissolved in H<sub>3</sub>PO<sub>4</sub> (100%), for 1 h at 70 °C in a  
130 sealed vial flushed with helium. The headspace gas (CO<sub>2</sub>) was entrained in a helium stream,  
131 automatically dried and purified and then injected into the continuous flow isotope ratio mass  
132 spectrometer via an active open split. Sample results were corrected using the international standard  
133 NBS-19 and a set of internal standards (two marbles, MOM and MS, and a carbonatite NEW12,  
134 previously calibrated using the international standards NBS-18 and NBS-19, e.g. Negri et al., 2015)  
135 and normalized to the V-PDB international standard and expressed in the well-known δ-notation.

136 All samples were analysed in duplicate and analytical uncertainties for replicated analyses of  $\delta^{18}\text{O}$   
137 and  $\delta^{13}\text{C}$  were  $\pm 0.15$  ‰ or better. The  $\delta^{18}\text{O}$  values of water are reported as V-SMOW.  
138

## 139 4. Results

### 140 4.1 The terrestrial mollusc assemblage

141 A very low number of terrestrial mollusc shells were recovered from the sampled sediments.  
142 These are all gastropods, no bivalves were found. Sample SUL-16/01 was virtually devoid of fossil  
143 remains, whereas sample SUL-16/02 contained less than 20 shells/kg. Despite the relatively low  
144 number of individuals, the counts can be considered representative for ecological analyses due to  
145 the amount of material sieved. All the shell remains belonged to terrestrial molluscs (Table 1), and  
146 only scarce fragments of unidentifiable micromammal bones were recovered.

147 Six species of terrestrial molluscs were recovered (Tab. 1; Fig. 3), two of which could not be  
148 identified to species level. The enid *Jaminia* sp. is represented by two shell apices only. As the  
149 extant species of this genus can be distinguished from the extinct Quaternary *Jaminia malatestae*  
150 (Esu, 1988) only based on the shell aperture it was not possible to identify these specimens to  
151 species level. The helicelline geomitrid, the most represented species in the paleosol, belongs to a  
152 group whose genus level taxonomy is entirely based on anatomical characters of the soft-parts.  
153 Therefore it was also not possible to make a more detailed taxonomic identification for this taxon.  
154 Shell features of the Sulmona geomitrid matched those of species in genera *Candidula*, *Cernuella*,  
155 *Helicella*, *Helicopsis*, *Xerocrassa* and *Xerosecta* (see the thorough iconographic survey on  
156 European species by Welter-Schultes, 2012). It could be hypothesized that the Fiorata Paleosol  
157 species corresponded to *Helicopsis striata* (Müller, 1774), a small European xerophilous geomitrid  
158 often associated with *Pupilla muscorum*.

159 From an ecological perspective, the identified species can be associated with dry to  
160 mesophilous open habitats (Tab. 1). *Pomatias elegans* is a medium-sized European prosobranch  
161 snail living among litter, humus and plant debris in many different dry to mesophilous habitats with  
162 some plant cover and preferably on calcareous substrates. *Truncatellina cylindrica* is a very minute  
163 European-Mediterranean pulmonate snail living among humus and leaf litter in dry to mesophilous  
164 habitats with some plant cover. The extant *Jaminia* species are small to medium-sized European  
165 calciphile pulmonates living on the soil surface or among rocks in dry, open grasslands and  
166 limestone reliefs. The Middle and Late Pleistocene *Jaminia malatestae* has been reported in open-  
167 dry paleoenvironments from the central-southern Italian peninsula during cold climatic periods (Di  
168 Vito et al., 1998; Marcolini et al., 2003; D'Amico and Esu, 2011; Limondine-Louzet et al., 2017).

169 *Pupilla muscorum* is a very small Holarctic pulmonate snail usually living among humus, leaf litter  
170 and rock debris in dry, cool, open habitats, preferably on calcareous substrates. *Vallonia costata* is a  
171 very small Holarctic snail, living among humus, litter, moss and plant debris in mesophilous open  
172 or sparsely vegetated habitats. This is also valid for the helicelline geometrid, which is typical of  
173 dry, open, sunny habitats (indeed its shell is a typical “chalconcha” following the shell  
174 classification by Sacchi, 1952).

#### 175 *4.2 Mineralogical and isotopic analyses*

176 The XRD analysis confirmed that the terrestrial shells preserved their primary aragonite  
177 mineralogy, as also suggested by their well-preserved aspect (Fig. 4b). Only one sample had a  
178 considerable amount of calcite (ca. ¼) and thus it was excluded from further isotopic analysis.  
179 However, we suspect that this was due to the presence of thin and superficial encrustations of  
180 pedogenic carbonates. Oxygen isotope composition of terrestrial shells ranged from - 4.26 ‰ to -  
181 2.55 ‰, whereas their carbon isotope composition ranged from - 9.42 ‰ to - 8.34 ‰ (Table 2).

182 Pedogenic carbonates were mm-sized, often elongated fine-grained concretions, preserving  
183 small cylindrical holes, sometimes ramified. Most were consistent with “hypocoatings-type” (Fig.  
184 4c) carbonate concretions (e.g. Barta, 2011). The XRD analysis indicated that the small pedogenic  
185 concretions were mostly formed of calcite, along with minor quartz inclusions and traces of  
186 feldspars and micas (Fig. 4a), as further confirmed by SEM-EDS. Microscopic investigations did  
187 not show clear evidence of several phases of calcite depositions supporting their origin as  
188 impregnations around pores (i.e. small roots) of the soil matrix (Barta, 2011). Oxygen isotope  
189 composition of pedogenic carbonates ranged from - 7.60 ‰ to - 6.54 ‰, whereas their carbon  
190 isotope composition ranged from - 10.02 ‰ to - 9.52 ‰ (Table 2).

191

## 192 **5. Discussion**

### 193 *5.1 Chronology and paleoenvironmental significance of the mollusc assemblage*

194 The deep unconformity at the base of SUL-5, which cuts up to ~50 m of the underlying unit  
195 SUL-6 (Figs. 1 and 2), filled by fluvial gravels and sands, and capped by the Fiorata Paleosol,  
196 indicates a pronounced and long phase of lake low-stand associated to the complete desiccation of  
197 the lacustrine system. Based on the available chronological and stratigraphic constraints (Figs. 1  
198 and 2), this subaerial phase can be roughly dated between ~650 ka and ~530 ka, or between MIS 16  
199 and MIS 14. However, the Fiorata Paleosol documents only the final stages of this long subaerial

200 phase, and the timing of the end of the soil-forming phase can be precisely constrained by the  
201 deposition of the thick tephra layer correlated to the Tufo di Bagni Albule, dated to  $527\pm 2$  ka (Fig.  
202 2). Recently, a tephra layer dated to  $531\pm 5$  ka, and tentatively correlated to the Tufo di Bagni  
203 Albule, has also been identified in the archaeological succession of Valle Giumentina (layer T109b,  
204 Villa et al., 2016), located  $\sim 15$  km NE of Sulmona Basin). According to the MIS chronology (e.g.  
205 Railsback et al., 2015), the Fiorata Paleosol can therefore be correlated with the period  
206 corresponding to MIS 14 (Fig. 2) and/or to the MIS 14-MIS 13 transition . However, the non-  
207 marine fauna is suggestive of an open-dry environment and more indicative of a glacial phase,  
208 better corresponding to a later phase of the glacial MIS 14.

209 The fauna is characterized by a low number of species and shares some general similarities with  
210 other terrestrial mollusc assemblages from the central Italian Peninsula considered typical of colder  
211 and drier conditions of glacial periods (e.g. Esu, 1981; Di Vito et al., 1998; Limondin-Lozouet et  
212 al., 2017; Boretto et al., 2017). Similarly, the terrestrial molluscs from Sulmona Basin indicate open  
213 and moderately dry habitats, as inferred from the presence of mesophilous and slightly  
214 thermophilous components (Table 1, i.e. *Pomatias elegans*). The presence of more thermophilous  
215 elements among the terrestrial molluscs correlated to glacial phases in the central Mediterranean,  
216 typically absent in coeval assemblages in central Europe, has already been noted by Sarti et al.  
217 (2005). This probably indicates the less extreme character, in terms of temperature, of these  
218 assemblages compared to the glacial counterparts of central to southern Europe. Interestingly, rare  
219 remains of *P. elegans* have also been found in the Valle Giumentina succession in the upper  
220 “glacial” assemblages (VG3 and VG4 biozones, Limondin-Lozouet et al., 2017), which for the  
221 generally low number of species (indicating dry and open habitats), resembles Fiorata Paleosol  
222 assemblage. However, VG3 and VG4 biozones are stratigraphically above the tephra dated to  
223  $531\pm 5$  ka at Valle Giumentina and tentatively correlated to the Tufo di Bagni Albule (unfortunately,  
224 there is no support chemical data for this layer), and therefore they do not precisely match the  
225 chronological interval documented by the Fiorata Paleosol. Conversely, the assemblages below the  
226 T109b tephra (VGM2 biozone) is characteristic of interglacial conditions, as documented by a  
227 larger number of species indicating forest environment and mild climate. As such we are inclined to  
228 conclude that the malacological record from Valle Giumentina is not chronologically synchronous  
229 with the Fiorata Paleosol assemblage (i.e. glacial MIS 14), therefore preventing a detailed  
230 correlation among the two records.

## 231 5.2 Stable isotope geochemistry

232 The shells and pedogenic carbonates have very distinctive  $\delta^{18}\text{O}$  and  $\delta^{13}\text{C}$  values (Fig. 4),

233 which also differ from the values obtained from lacustrine carbonates dated to MIS 11 and MIS 12  
234 in the same basin (Regattieri et al., 2016), as well from clastic marine carbonates from the  
235 substratum (Regattieri et al., 2016; Villa et al., 2016). Along with the mineralogical evidence for the  
236 preservation of the shell mineralogy, the isotopic distribution provides robust evidence that  
237 terrestrial carbonates were not isotopically altered by diagenesis. This also indicates that pedogenic  
238 carbonates were not significantly contaminated by clastic carbonate.

239 Aragonite is usually enriched in  $^{18}\text{O}$  and  $^{13}\text{C}$  compared to calcite (Tarutani et al., 1969;  
240 Grossman and Ku, 1986; Romanek et al., 1992; Kim and O'Neil, 1997), but the difference observed  
241 between pedogenic carbonates and shells is not simply related to different isotopic fractionation  
242 factors. Terrestrial shells have  $\delta^{13}\text{C}$  values higher than pedogenic carbonate by ca. 1 ‰. This value  
243 is slightly lower than those expected for calcite and aragonite precipitating close to isotopic  
244 equilibrium from the same solution (ca. 1.7 ‰, Romanek et al. 1992). We noticed, however, that  
245 analyses of aragonite and calcite in biogenic carbonates yielded differences in values closer to ca. 1  
246 ‰ (Lécuyer et al., 2012). The  $\Delta$  ( $\delta^{18}\text{O}_{\text{aragonite}} - \delta^{18}\text{O}_{\text{calcite}}$ ) values show some differences according to  
247 the equations used (e.g. usually lower than 1 ‰, Tarutani et al., 1969; Grossman and Ku, 1986;  
248 Patterson et al., 1993; Kim and O'Neil, 1997; Lécuyer et al., 2012), but these differences are always  
249 lower than those observed between the  $\delta^{18}\text{O}$  of aragonitic shells and pedogenetic carbonates in our  
250 record (ca. 4 ‰, Fig. 4). This difference can be explained by kinetic (vital) offset compared to  
251 equilibrium conditions for terrestrial mollusc shells, and to different environmental water sources  
252 from which the two carbonate polymorphs precipitate (i.e. the shell and the pedogenic carbonate).

253 The  $\delta^{18}\text{O}$  values of terrestrial gastropod shells is proven to be related to the  $\delta^{18}\text{O}$  values of  
254 environmental waters absorbed/ingested by the snails (e.g. water vapour, dew, local meteoric  
255 precipitation, e.g. Lécolle, 1985; Goodfriend et al., 1989; Zanchetta et al., 2005; Prendergast et al.,  
256 2015), and to isotopic effects linked to the exchange of fluid between the external environment  
257 (through the body of the snails) and internal fluid (Balakrishnan and Yapp, 2004), which are  
258 influenced by relative humidity (Balakrishnan and Yapp, 2004) and temperature. Therefore, no  
259 simple isotopic equilibrium with meteoric water could be assumed. However, empirical relations  
260 between the  $\delta^{18}\text{O}$  values of meteoric water and the shells have been found within living populations  
261 (e.g. Lécolle, 1985; Goodfriend and Ellis, 2002; Zanchetta et al., 2005; Yanes et al., 2008;  
262 Prendergast et al., 2015), although in very arid lands a direct correlation is often not particularly  
263 robust (Goodfriend et al., 1989). Considering the data available from different living populations,  
264 there is no conclusive evidence that oxygen isotopic composition of shells is species-dependent  
265 (e.g. Lécolle, 1985; Goodfriend and Ellis, 2002; Zanchetta et al., 2005; Baldini et al., 2007; Yanes  
266 et al., 2008, 2009; Colonese et al., 2013ab, 2014). However, some significant differences have been



267 reported in the literature in oxygen isotope composition between land snail populations living in the  
268 same place (Goodfriend and Magaritz, 1987; Yanes et al., 2011). Rather than a real species offset,  
269 these differences could be related to factors like duration of activity, life cycle, use of different  
270 water sources (dew, ingested food, rainfall) and/or the time of shell deposition compared to life  
271 cycle (e.g. Goodfriend and Magaritz, 1987). Ecological niches, occupied by different populations  
272 living in the same site, can additionally influence the final oxygen isotope composition of the shells  
273 (Goodfriend et al., 1989; Balakrishnan et al., 2005b; Yanes et al., 2008, 2009; Colonese et al.,  
274 2013b, 2014). The most complete model to interpret oxygen isotope composition of terrestrial  
275 gastropod shells, assuming no species offset, is that proposed by Balakrishnan and Yapp (2004).  
276 The model indicates that the steady-state  $\delta^{18}\text{O}$  value of shell carbonate depends upon temperature,  
277 relative humidity,  $\delta^{18}\text{O}$  of the input liquid water and  $\delta^{18}\text{O}$  of ambient water vapour. However,  
278 quantitative prediction using this model involves several assumptions, which complicate its  
279 applicability to past samples (Balakrishnan et al., 2005a; Colonese et al., 2013a).  
280 For living populations in Italy, Zanchetta et al. (2005) found an empirical relation between isotopic  
281 composition of precipitation ( $\delta^{18}\text{O}_p$ ) and isotopic composition of shell ( $\delta^{18}\text{O}_s$ ):

282

$$283 \delta^{18}\text{O}_p = 0.65 \times \delta^{18}\text{O}_s + 5.44 \quad (r^2 = 0.79) \quad (1)$$

284

285 If relation (1) is assumed valid also for the past and for Sulmona settings, the average values of the  
286 oxygen isotope composition of meteoric water during the period of shell calcification can be  
287 calculated to be  $-7.8 \pm 0.5$  ‰.

288 Oxygen isotope composition of pedogenic carbonate is mostly related to local rainfall (Cerling,  
289 1984), with additional evaporative effects in the soil and the effect of temperature-related isotopic  
290 fractionation during calcite precipitation. Using Cerling's (1984) data on modern soils, Jiamao et al.  
291 (1997) proposed the following relationship between  $\delta^{18}\text{O}$  values in water and soil carbonate, which  
292 incorporates the evaporative effect in soils (Zanchetta et al., 2000) and the effect of the temperature  
293 in the fractionation factor:

294

$$295 \delta^{18}\text{O}_p = -1.361 + 0.955 \times \delta^{18}\text{O}_{\text{CaCO}_3} \quad (r^2 = 0.98) \quad (2)$$

296

297 Boretto et al. (2017) found that equation (2) is a good predictor of isotopic composition of current  
298  $\delta^{18}\text{O}_p$  along the Tuscan coast. Assuming that equation (2) can also be applied to older pedogenic

299 carbonates, it provides an average  $\delta^{18}\text{O}$  precipitation value of  $\approx 8.3 \pm 0.4$  ‰. This  $\delta^{18}\text{O}$  value is  
300 similar, though lower, to those obtained from the Fiorata Paleosol shells, a fact that mutually  
301 supports the two estimations. We note that the equations (1) and (2) have been obtained using the  
302 annual average  $\delta^{18}\text{O}$  value of local rainfall, so in principle the calculated values should be  
303 interpreted accordingly. However, terrestrial molluscs form their shells predominantly during wetter  
304 and/or warmer conditions (Balakrishnan and Yapp, 2004), therefore, the isotopic signal would be  
305 skewed toward the growth period (Kehrwald et al., 2010). If the warmer part of the year (e.g.  
306 spring/summer) was the principal season for the shell growth, higher  $\delta^{18}\text{O}$  values of meteoric  
307 precipitation would be expected (Rozanski et al., 1993; Fricke and O'Neil, 1999) as, indeed,  
308 observed. Today in the Mediterranean, during the hottest part of summer land snails aestivate (e.g.  
309 Yurena et al., 2011), and are mostly active during spring and early autumn. However, during  
310 periods with a potentially cooler and wetter climate (i.e., glacial events), summer would be the  
311 greatest period of activity for land snails.

312 While pedogenic carbonates may precipitate from soil water which is more representative of  
313 the annual average recharge conditions (Cerling, 1984), Breecker et al. (2009) observed that  
314 pedogenic carbonates in very dry environments form during warmer, drier periods and from soil  
315 solution mostly recharged during wetter periods. If the soil water solution from which carbonate  
316 precipitates represents the colder months of recharge, this would explain the lower estimated  $\delta^{18}\text{O}$   
317 for precipitation compared to that obtained for shells. On the other hand, pedogenic carbonates can  
318 be the result of repeated events of carbonate deposition (and eventually re-dissolution), and thus  
319 their isotopic composition represents the weighted average of multiple events over a certain period  
320 of time. The mm-size of hypocoatings (Fig. 4c), and absence of clear evidence of phases of growth  
321 and dissolution, suggest that they form over a relatively short time (less than centuries, e.g.  
322 Retallack, 2005). Similarly, shells dispersed within soil horizons are not necessarily coeval, but may  
323 represent a different period of burial. All these factors can complicate the proposed interpretation,  
324 however, the relatively narrow  $\delta^{18}\text{O}$  values measured also suggest that conditions did not change  
325 significantly during the soil formation.

326 The most striking feature is that the estimated  $\delta^{18}\text{O}$  values of precipitation are, on average,  
327 lower than the values measured today at L'Aquila station ( - 7.13 ‰), also considering a small  
328 altitudinal correction for the Sulmona basin (ca. - 0.15 ‰). Lower  $\delta^{18}\text{O}$  of precipitation during  
329 glacial/stadial conditions is expected at latitudes where isotopic composition of meteoric  
330 precipitation is strongly related to temperature (Rozanski et al., 1993). In the central Mediterranean  
331 a dependence between precipitation  $\delta^{18}\text{O}$  and surface temperature ( $\delta^{18}\text{O}/T$ ) has been found to be ca.

332 +0.2 ‰/°C, and this relation can be assumed also for the last two glacial periods (Bard et al., 2002).  
333 Therefore, the differences between present day  $\delta^{18}\text{O}$  values of precipitation and the predicted  
334 average  $\delta^{18}\text{O}$  value from pedogenic carbonates would account for ca. 5°C lower temperature at the  
335 time of soil carbonate formation, perhaps representing winter recharge; whereas the Fiorata  
336 Paleosol shells indicate less than 3°C lower temperature, probably due to expression of the warmer  
337 season.

338 It has been suggested that in the central Mediterranean most of the  $\delta^{18}\text{O}$  signal in Quaternary  
339 continental carbonates is dominated by the “amount effect” of rainfall (ca. - 2 ‰/100 mm; Bard et  
340 al., 2002). This assumption has been used specifically for lakes for which additional evaporative-  
341 enrichment effects have been suggested during drier periods (Zanchetta et al., 1999,2007a; Roberts  
342 et al., 2008; Giaccio et al., 2015; Regattieri et al., 2015,2016), and for speleothem carbonate (Bar-  
343 Matthews et al., 2000; Regattieri et al., 2014; Zanchetta et al., 2007a,2016), for which the  
344 evaporative effect could be considered minor. Oxygen isotope composition of authigenic, bio-  
345 mediated calcite from lacustrine intervals from the Sulmona Basin unequivocally indicate that  
346 carbonates tend to have higher  $\delta^{18}\text{O}$  values during colder and drier periods (Regattieri et al.,  
347 2015,2016,2017; Giaccio et al., 2015). Higher  $\delta^{18}\text{O}$  values of lacustrine calcite during colder and  
348 drier periods at Sulmona probably result from the combination of several factors. During a glacial  
349 period  $^{16}\text{O}$ -enriched water is stored in continental ice (the “ice volume effect”, e.g. Mix and  
350 Ruddiman, 1984) leading to  $^{18}\text{O}$ -enriched ocean waters; this enrichment is propagated into the  
351 hydrological cycle. The most obvious local effect is the lower temperature of carbonate  
352 precipitation, with related changes in the fractionation factor (Kim and O’Neil, 1997 and references  
353 therein), even though the occurrence of algal blooms responsible for calcite precipitations cannot  
354 occur for too lower temperatures. Moreover, drier conditions during glacial periods could enhance  
355 evaporation, causing enrichment in  $^{18}\text{O}$  in residual water (Gonfiantini, 1986).

356 While environmental conditions derived from the terrestrial mollusc assemblages and from  
357 the general stratigraphic features are consistent with a general reduction in the amount of  
358 precipitation, both shell and pedogenic carbonates predict considerably lower  $\delta^{18}\text{O}$  values in  
359 meteoric precipitation. This clearly challenges the assumption that the rainfall amount exerts a  
360 dominant effect on the isotopic composition of continental carbonates in the Mediterranean area, at  
361 least for the interval considered.

362 A possible explanation to reconcile these discordant interpretations is that terrestrial  
363 carbonates show distinct responses to precipitation regimes. Lakes and speleothems tend to have  
364 recharge systems that average and mix rainfall over the catchment area, and thus are more sensitive

365 to the total amount of precipitation. Terrestrial gastropod shells, instead, are more susceptible to  
366 local precipitation and humidity during the period of growth. Pedogenic carbonates would be more  
367 sensitive to local rainfall and specific periods of recharge of soil interstitial water. For instance, the  
368 pedogenic carbonates of the Fiorata Paleosol would have been influenced by a shift in large-scale  
369 atmospheric circulation. This may have taken the form of frequent incursions of cold air masses,  
370 depleted in  $^{18}\text{O}$ , deriving from northern latitudes of continental Europe, producing mostly snow  
371 precipitation (Enzi et al., 2014). Melting snow can have a different soil infiltration pattern  
372 compared to rainfall. This may have led to carbonates mostly recharged by  $^{18}\text{O}$ -depleted waters.  
373 Shells may have formed during warmer parts of the year but during wetter precipitation events  
374 characterised by particularly lower-than-average  $\delta^{18}\text{O}$  values (e.g. Colonese et al., 2007, 2013).

375 It is important to emphasize that the empirical equations discussed herein may not be widely  
376 applicable to past climates, in particular for glacial periods for which different synoptical climate  
377 conditions would have existed (Kuhleemann et al., 2008; Kehrwald et al., 2010).

378 On the other hand, the MIS 14 is a particularly weak glacial in many records (Lang and Wolff,  
379 2011), as shown by the global benthic stack of Lisieki and Raymo (2005) or ice core temperatures  
380 (Jouzel et al., 2007). The pollen record at Thenaghi Philippon in Greece did not show a very  
381 prominent decrease in arboreal vegetation for MIS 14, even though phases of increased grasses due  
382 to drier and colder conditions were recognized (Tzedakis et al., 2006). This is also evident in Lake  
383 Ohrid where MIS 14 seems one of the less expressed glacial periods of the record (Franke et al.,  
384 2016).

385 Carbon isotope composition of both shells and pedogenic carbonates is indirectly related to  
386 vegetation cover, but with different and complex relationships. Terrestrial molluscs form their shells  
387 mainly from respired  $\text{CO}_2$ , and shell  $\delta^{13}\text{C}$  values mostly reflect the stable carbon isotope  
388 composition of ingested vegetation (e.g. Goodfriend et al., 1989; Stott, 2002; Metref et al., 2003;  
389 Balakrishnan et al., 2005b; Liu et al., 2007; Prendergast et al., 2017). However, depending on the  
390 species and environmental settings (calcareous areas) shell  $\delta^{13}\text{C}$  values may also be affected by the  
391 ingestion of soil carbonates (Yates et al., 2002; Romaniello et al., 2008; Yanes et al., 2008;  
392 Colonese et al., 2014). Moreover, different feeding behavior and food preferences may variably  
393 affect shell  $\delta^{13}\text{C}$  values (Colonese et al., 2014). Using vegetation as the unique  $\text{CO}_2$  source for shell  
394 carbon isotopes, Stott (2002) found a strong positive linear relationship between plant and shell  
395  $\delta^{13}\text{C}$  ( $\delta^{13}\text{C}_{\text{shell}}$ ):

396  
397 
$$\delta^{13}\text{C}_{\text{diet}} = 1.35 \times \delta^{13}\text{C}_{\text{shell}} - 11.73 \quad (3)$$

399 The equation (3) has been obtained for *Cornu aspersum* and the applicability to other species might  
 400 be questionable. However, applied to our shell  $\delta^{13}\text{C}$  values, it provides an average value for the  
 401 ingested food of  $-23.7 \pm 0.6$  ‰. The average value for  $\text{C}_3$  plants is ca.  $-27$  ‰ (e.g. Deines, 1980),  
 402 and the calculated values of ingested vegetation are consistent with carbon isotope values obtained  
 403 from  $\text{C}_3$  vegetation from moderately dry conditions. Carbon isotope composition of  $\text{C}_3$  vegetation in  
 404 drier environments can be significantly higher than plants from wet environments (e.g. Kohn,  
 405 2010). Specifically in the Mediterranean, remarkable differences in  $\delta^{13}\text{C}$  of  $\text{C}_3$  plants are observed  
 406 related to changes in water-use efficiency, which also varies largely between species, with higher  
 407  $^{13}\text{C}/^{12}\text{C}$  ratio measured in drier areas (Hartman and Danin, 2010; Prendergast et al., 2017).  
 408 Moreover, in the Mediterranean area similar shell  $\delta^{13}\text{C}$  values have been reported in ecosystems  
 409 dominated by  $\text{C}_3$  plants (Goodfriend et al., 1989; Colonese et al., 2014; Prendergast et al., 2015).

410 For pedogenic carbonates there are theoretical equations which can be applied for  
 411 calculating the  $\delta^{13}\text{C}$  values of vegetation from which it is precipitated and the relative amount of  $\text{C}_3$   
 412 and  $\text{C}_4$  vegetation. According to Wang and Zheng (1989) the  $\delta^{13}\text{C}$  values of vegetation over a soil  
 413 can be estimated from the carbon isotope composition of pedogenic carbonate, with the following  
 414 equation:

$$415 \quad x = (11.9 + \delta^{13}\text{C}_{\text{pedogenic}}) / 14 \quad (4)$$

418 Applying the equation (4) to our carbonate  $\delta^{13}\text{C}$  values, a proportion of  $\text{C}_4$  plants ranging from 30  
 419 to 38 % is obtained.  $\text{C}_4$  vegetation is relatively rare in southwestern Europe and mostly belonging to  
 420 herb and shrubs (Pyankov et al., 2010), as such these estimations seem particularly high. Indeed,  
 421 these estimations are based on the assumption that  $\text{C}_3$  plants have a mean carbon isotopic value of  
 422 ca.  $-27$  ‰, which is only a first-order estimation, whereas higher values of prevailing  $\text{C}_3$  vegetation  
 423 can be obtained by water stress, as previously discussed.

424 Considering the  $\text{C}_4$  estimation from the isotopic composition of pedogenic carbonate, Breecker et  
 425 al. (2009) observed that in dry environments pedogenic carbonates form predominantly during  
 426 warm and dry conditions, and during periods of low soil respired- $\text{CO}_2$ , thus overestimating the  
 427 presence of  $\text{C}_4$  vegetation. This supports the observation obtained from shell  $\delta^{13}\text{C}$  values that the  
 428 relatively high  $\delta^{13}\text{C}$  values in pedogenic carbonates at Sulmona derive from  $\text{C}_3$  vegetation enriched  
 429 in  $^{13}\text{C}$  during dry seasons. The integration of these two sources of paleoenvironmental information  
 430 offers stronger arguments for interpreting past vegetation cover during soil formation, notably in  
 431 Mediterranean areas, where the isotope ecology of modern and fossil shells is relatively well  
 432 known.

433

## 434 **6. Conclusion**

435 Chronological, stratigraphic, and paleontological data indicate that the paleosol at the base of  
436 SUL5 in the Sulmona Basin sedimentary succession was formed during drier and probably colder  
437 conditions at the time of the MIS 14 glacial phase. The local mollusc assemblage indicates an open,  
438 dry environment. Carbon isotope compositions of pedogenic carbonates and shells consistently  
439 suggest prevailing C<sub>3</sub> vegetation adapted to dry environments. Inferred oxygen isotope composition  
440 of past rainfall from shells and pedogenic carbonates indicates that precipitation was generally <sup>18</sup>O-  
441 depleted over the region compared to present-day. While this could imply a decrease in the  
442 atmospheric temperature of ca. 3-5°C compared to present day, this also conflicts with the current  
443 interpretation of speleothems and lake δ<sup>18</sup>O values in the central Mediterranean. For example, lower  
444 δ<sup>18</sup>O values in carbonates (arising from lower precipitation δ<sup>18</sup>O values) should reflect increased  
445 rainfall, due to the amount effect. But increased rainfall is not supported in our record according to  
446 the paleontological data and/or the carbon isotope composition of carbonates. We propose that more  
447 frequent incursions of <sup>18</sup>O-depleted cold air masses deriving from northern latitudes of continental  
448 Europe, along with a general context of reduced precipitation, would have influenced the isotopic  
449 composition of pedogenic carbonates and terrestrial shells. This work highlights the importance of  
450 integrating isotopic approaches on terrestrial carbonates (molluscs and pedogenic carbonates) to  
451 derive more robust interpretative frameworks on past climate and environments in the  
452 Mediterranean region.

453

## 454 **Acknowledgments**

455 This study has been financially supported by Fondi di Ateneo and Laboratorio di  
456 Paleoclimatologia (University of Pisa, Leader G. Zanchetta), within the frame of multidisciplinary  
457 research in the Central Mediterranean for defining past climatic changes. ER is supported by project  
458 SFB806 "Our way to Europe". The authors thank Krista McGrath for reviewing the English. The  
459 authors also thank A. Prendergast and an anonymous reviewer for their constructive comments,  
460 which improved the quality of the manuscript.

461

## 462 **References**

463

464 Balakrishnan, M., Yapp, C.J., 2004. The flux balance model for the oxygen and carbon isotope

465 compositions of land snail shells. *Geochem. Cosmochim. Acta* 68, 2007–2024.  
466  
467 Balakrishnan, M., Yapp, C.J., Meltzer, D.J., Theler, J.L., 2005a. Paleoenvironmental of the Folsom  
468 archeological site, New Mexico, USA, approximately 10,500 <sup>14</sup>C yr B.P. as inferred from stable  
469 isotope composition of fossil land snail shells. *Quat. Res.* 63, 31–44.  
470  
471 Balakrishnan, M., Yapp, C.J., Theler, J.L., Carter, B.J., Wyckoff, D.G., 2005b. Environmental  
472 significance of <sup>13</sup>C/<sup>12</sup>C and <sup>18</sup>O/<sup>16</sup>O ratios of modern land-snail shells from southern great plains of  
473 North America. *Quat. Res.* 63, 15–30.  
474  
475 Baldini, M.L., Walzer, S.E., Railsback, L.B., et al. 2007. Isotopic ecology of the modern land snail  
476 *Cerion*, San Salvador, Bahamas: Preliminary advances toward establishing a low-latitude island  
477 paleoenvironmental proxy. *Palaios* 22, 174–187.  
478  
479 Barbieri, M., Boschetti, T., Petitta, M., Tallini, M., 2005. Stable isotopes (<sup>2</sup>H, <sup>18</sup>O and <sup>87</sup>Sr/<sup>86</sup>Sr) and  
480 hydrochemistry monitoring for groundwater hydrodynamics analysis in a karst aquifer (Gran Sasso,  
481 Central Italy). *Appl. Geochem.* 20, 2063–2081.  
482  
483 Bard, E. Delaygue, G. Rostek, F. Antonioli, F. Silenzi, S. Schrag, D., 2002. Hydrological conditions  
484 in the western Mediterranean basin during the deposition of Sapropel 6 (ca. 175 kyr), *Earth Planet.*  
485 *Sci. Lett.* 202 (2002) 481– 494.  
486  
487 Bar-Matthews, M., Ayalon, A., Kaufmann, A., 2000. Timing and hydrological conditions of  
488 sapropel events in the eastern Mediterranean, as evident from speleothems, Soreq cave, Israel.  
489 *Chem. Geol.*, 169, 145–156, 2000.  
490  
491 Barta, G., 2011. Secondary carbonates in loess-paleosoil sequences: a general review. *Centr. Europ.*  
492 *J. Geoscienc.* 3/2, 129-146.  
493  
494 Boretto, G., Zanchetta, G., Ciulli, L., Bini, M., Fallick, A.E., Lezzerini, M., Colonese, A.C.,  
495 Zembo, I., Trombino, L., Regattieri, E., Sarti, G., 2017. The loess deposits of Buca dei Corvi  
496 section (central Italy): revisited. *Catena*, 151, 225-237.  
497  
498 Bouchet, P., Rocroi, J.-P., 2005. Classification and nomenclator of gastropod families. *Malacologia*  
499 47, 1-397.

500

501 Breecker, D.O., Sharp, Z.D., McFadden, L.D. 2009. Seasonal bias in the formation and stable  
502 isotopic composition of pedogenic carbonate in modern soils from central New Mexico, USA. GSA  
503 Bull. 121, 630–640.

504

505 Bruker, AXS Inc. (2015) DIFFRAC.EVA. Bruker Advanced X-ray Solutions, Madison, Wisconsin,  
506 USA.

507

508 Cavinato G.P., Miccadei, E. 2000. Pleistocene carbonate lacustrine deposits: Sulmona basin (central  
509 Apennines, Italy). In: Gierlowsky-Kordesch, E.H., Kelts, K.R. (eds) “Lake Basins Through Space  
510 and Time.” Studies in Geology, Am. Ass. Petrol. Geol. 46, 517–526.

511

512 Cerling, T.E., 1984. The stable isotopic composition of modern soil carbonate and its relationship to  
513 climate. Earth Planet. Sc. Lett. 71, 229–240.

514

515 Cerling, T.E., Quade, J. 1993. Stable carbon and oxygen isotopes in soil carbonates. In Climate  
516 Change in Continental Isotopic Records, Swart PK, Lohmann KC, McKenzie JA, Savin S. (eds).  
517 American Geophysical Union, Geophys. Monogr. 78, 217–231.

518

519 Colonese, A.C., Zanchetta, G., Fallick, A.E., Martini, F., Manganelli, G., Drysdale, R.N., 2010.  
520 Stable isotope composition of *Helix ligata* (Müller, 1774) from Late Pleistocene- Holocene  
521 archaeological record from Grotta della Serratura (Southern Italy): Palaeoclimatic implications.  
522 Glob. Planet. Change 71, 249–257.

523

524 Colonese, A.C., Zanchetta, G., Fallick, A.E., Martini, F., Manganelli, G., Lo Vetro, D., 2007. Stable  
525 isotope composition of Late Glacial land snail shells from Grotta del Romito (Southern Italy):  
526 palaeoclimatic implications. Palaeogeogr., Palaeoclimat., Palaeoecol. 254, 550–560.

527

528 Colonese, A.C., Zanchetta, G., Fallick, A.E., Manganelli, G., Saña, M., Alcade, G., Nebot, J.,  
529 2013a. Holocene snail shell isotopic record of millennial-scale hydrological conditions in western  
530 Mediterranean: Data from Bauma del Serrat del Pont (NE Iberian Peninsula). Quat. Int. 303, 43-53.

531



532 Colonese, A.C., Zanchetta, G., Perlès, C., Drysdale, R.N., Manganelli, G., Baneschi, I., Dotsika, E.,  
533 Valladas, H., 2013b. Deciphering late Quaternary land snail shell  $\delta^{18}\text{O}$  and  $\delta^{13}\text{C}$  from Franchthi  
534 Cave (Argolid, Greece). *Quat. Res.* 80, 66-75.

535

536 Colonese, A.C., Zanchetta, G., Fallick, A.E., Manganelli, G., Lo Cascio, P., Hausmann, N.,  
537 Baneschi, I., Regattieri, E. 2014. Oxygen and carbon isotopic composition of modern terrestrial  
538 gastropod shells from Lipari Island, Aeolian Archipelago (Sicily). *Palaeogeogr., Palaeoclimatol.,*  
539 *Palaeoecol.* 394, 119–127.

540

541 D’Amico, C., Esu, D., 2011. *Jaminia (Jaminia) malatestae* Esu, 1988 (Mollusca, Gastropoda,  
542 Enidae) from the Middle and Late Pleistocene of central-southern Italy. palaeoecological  
543 implications. *Il Quaternario, Italian Journal of Quaternary Sciences*, 24, 67-74.

544

545 Deines, P. 1980. The isotopic composition of reduced organic carbon. In P. Fritz and J.Ch. Fontes:  
546 *Handbook of Environmental Isotope Geochemistry*. 1, 329-406. Elsevier.

547

548 Di Vito, M., Sulpizio, R., Zanchetta, G. 1998. I depositi ghiaiosi della valle dei torrenti Clanio e  
549 Acqualonga (Campania centro-orientale): significato stratigrafico e ricostruzione paleoambientale.  
550 *Il Quaternario, Italian Journal of Quaternary Sciences*. 11, 273-286.

551

552 Enzi, S., Bertolin, C., Diodato, N., 2014. Snowfall time-series reconstruction in Italy over the last  
553 300 years. *The Holocene* 24, 346–356.

554

555 Esu, D., 1981. Significato paleoecologico e paleoclimatico di una malacofauna continentale  
556 pleistocenica dell’Italia centro-meridionale (Isernia, Molise). *Boll. Soc. Geol. It.*, 100, 93-98.

557

558 Fricke, H.C., O’Neil, J.R., 1999. The correlation between  $^{18}\text{O}/^{16}\text{O}$  ratios of meteoric water and  
559 surface temperature: its use in investigating terrestrial climate change over geologic time. *Earth*  
560 *Planet. Sc. Lett.* 170, 181–196.

561

562 Galli, P., Giaccio, B., Peronace, E., et al. 2015. Holocene paleoearthquakes and Early-Late  
563 Pleistocene slip-rate on the Sulmona Fault (Central Apennines, Italy). *Bulletin of the Seismological*  
564 *Society of America* 105: 1-13.

565

566 Giaccio, B., Nomade, N., Wulf, S., Isaia, R., Sottili, G., Cavuoto, G., Galli, P., Messina, P.,  
567 Sposato, A., Sulpizio, R., Zanchetta, G., 2012. The late MIS 5 Mediterranean tephra markers: a  
568 reappraisal from peninsular Italy terrestrial records. *Quat. Sc. Rev.*, 56, 31-45.  
569

570 Giaccio, B., Arienzo, I., Sottili, G., Castorina, F., Gaeta, M., Nomade, S., Galli, P., Messina, P.  
571 2013a. Isotopic (Sr and Nd) and major element fingerprinting of distal tephra: an application to the  
572 Middle-Late Pleistocene markers from the Colli Albani volcano, central Italy. *Quat. Sc. Rev.* 67,  
573 190-206.  
574

575 Giaccio, B., Castorina, F., Nomade, S., et al. 2013b. Revised chronology of the Sulmona lacustrine  
576 succession, central Italy. *J. Quat. Sc.* 28, 545–551.  
577

578 Giaccio, B., Regattieri, E., Zanchetta, G., Nomade, S., Renne, P.R., Sprain, C.J., Drysdale, R.N.,  
579 Tzedakis, P.C., Messina, P., Scardia, G., Sposato, A., Bassinot, F., 2015. Duration and dynamics of  
580 the best orbital analogue to the present interglacial. *Geology*, 43, 603–606.  
581

582 Giustini, F., Brilli, M., Patera, A., 2016. Mapping oxygen stable isotopes of precipitation in Italy. *J.*  
583 *Hydrol.* 8, 162–181.  
584

585 Gonfiantini, R., 1986. Environmental isotopes in lake studies. In P. Fritz and J. Ch. Fontes, Eds.  
586 “Handbook of Environmental Isotope Geochemistry”, Vol. 2, pp. 113–168. Elsevier, Amsterdam.  
587

588 Goodfriend, G.A., Ellis, G.L., 2002. Stable carbon and oxygen isotopic variations in modern  
589 *Rabdotus* land snail shells in the southern Great Plains, USA, and their relation to environment.  
590 *Geochim. Cosmochim. Acta* 66, 1987–2002.  
591

592 Goodfriend, G.A., Magaritz, M., 1987. Carbon and oxygen isotope composition of shell carbonate  
593 of desert land snails. *Earth. Planet. Sc. Lett.* 86, 377-388.  
594

595 Goodfriend, G.A., Magaritz, M., Gat, J.R., 1989. Stable isotope composition of land snail body  
596 water and its relation to environmental water and shell carbonate. *Geochim. Cosmochim. Acta* 53,  
597 3215–3221.  
598

599 Grossman, E.L., Ku, T.-L., 1986. Oxygen and carbon isotope fractionation in biogenic aragonite:  
600 temperature effects. *Chem. Geol. (Isotope Geosci. Sect.)* 59, 59–74.  
601

602 Hartman, G., Danin, A., 2010. Isotopic values of plants in relation to water availability in the  
603 Eastern Mediterranean region. *Oecologia* 162, 837–852.

604

605 Hassan M.K. 2015. Stable isotopic signatures of the modern land snail *Eremina desertorum* from a  
606 low-latitude (hot) dry desert - A study from the Petrified Forest, New Cairo, Egypt. *Chemie der*  
607 *Erde*, 75, 65–72.

608

609 Kerney, M.P., 1976. Mollusca from an interglacial tufa in East Anglia, with the description of a new  
610 species of *Lyrodiscus* Pilsbry (Gastropoda: Zonitidae). *J. Conchol.*, 29, 47–50.

611

612 Kehrwald, N.M., McCoy, W.D., Thibeault, J., Burns, S.J., Oches, E.A., 2010. Paleoclimatic  
613 implications of the spatial patterns of modern and LGM European land snail shell  $\delta^{18}\text{O}$ . *Quat. Res.*  
614 74, 166–176.

615

616 Kim, S.-T., O'Neil, J.R., 1997. Equilibrium and nonequilibrium oxygen isotope effects in synthetic  
617 carbonates. *Geochim. Cosmochim. Acta* 61, 3461–3475.

618

619 Kohn, M.J., 2010. Carbon isotope compositions of terrestrial  $\text{C}_3$  plants as indicators of  
620 (paleo)ecology and (paleo)climate. *PNAS*, 107, 19691–19695.

621

622 Kuhlemann, J., Rohling, E. J., Krumrei, I., Kubik, P., Ivy-Ochs, S., Kucera, M., 2008. Regional  
623 synthesis of Mediterranean atmospheric circulation during the Last Glacial Maximum. *Science*,  
624 321, 1338-1340.

625

626 Jiamao, H., Keppens, E., Tungsheng, L., Paepe, R., Wenyng, J. 1997. Stable isotope composition of  
627 the carbonate concretion in loess and climate change. *Quat. Int.* 37, 37–43.

628

629 Jouzel, J., Masson-Delmotte, V., Cattani, O., Dreyfus, G., Falourd, S., Hoffmann, G., Minster, B., J.  
630 Nouet, J., Barnola, J. M., Chappellaz, J., Fischer, H., Gallet, J. C., Johnsen, S., Leuenberger, M.,  
631 Loulergue, L., Luethi, D., Oerter, H., Parrenin, F., Raisbeck, G., Raynaud, D., Schilt, A.,  
632 Schwander, J. Selmo, E., Souchez, R., Spahni, R., Stauffer, B., Steffensen, J. P., Stenni, B.,  
633 Stocker, T. F., Tison, J. L. Werner, M. E., Wolff, W., 2007. Orbital and millennial Antarctic  
634 climate variability over the past 800,000 years. *Science*, 317, 793–796.

635

636 Lang, N., Wolff, E.W. 2011. Interglacial and glacial variability. *Clim. Past*, 7, 361–380.

637

638 Lécalle, P., 1985. The oxygen isotope composition of landsnail shells as climatic indicator:  
639 application to hydrogeology and paleoclimatology. *Chem. Geol., Isot. Geosci.* 58, 157– 181.

640

641 Lécuyer, C., Hutzler, A., Amiot, R., Daux, V., Grosheny, D., Otero, O., Martineau, F., Fourel, F.,  
642 Balter, V., Reynard, B. 2012. Carbon and oxygen isotope fractionations between aragonite and  
643 calcite of shells from modern molluscs. *Chem. Geol.* 332–333, 92–101

644

645 Leone, G., Bonadonna, F.P., Zanchetta, G., 2000. Stable isotope record in mollusca and pedogenic  
646 carbonate from Late Pliocene soils of Central Italy. *Palaeoclimatol., Palaeogeogr., Palaeoecol.*, 163,  
647 115-131.

648

649 Limondin-Lozouet, N., Antoine, P., 2006. A new *Lyrodiscus* (Mollusca, Gastropoda) assemblage  
650 from Saint-Acheul (Somme Valley): a reappraisal of MIS 11 malacofaunas from northern France.  
651 *Boreas*, 35, 622-633.

652

653 Limondin-Lozouet, N., Preece, R.C., 2004. Molluscan successions from the Holocene tufa of St-  
654 Germain-le-Vasson in Normandy, France. *J. Quat. Sc.* 19, 55-71.

655

656 Limondin-Lozouet, N., Villa, V., Pereira, A., Nomade, S., Bahain, J., Stoetzel, E., Aureli, D.,  
657 Nicoud, E. 2017. Middle Pleistocene molluscan fauna from the Valle Giumentina (Abruzzo, Central  
658 Italy): palaeoenvironmental, biostratigraphical and biogeographical implications. *Quat. Sc. Rev.*,  
659 156, 135-149.

660 Lisiecki, L.E., Raymo, M.E. 2005. A Pliocene-Pleistocene stack of 57 globally distributed benthic  
661  $\delta^{18}\text{O}$  records, *Paleoceanography*, 20, PA1003.

662

663 Liu, Z.X., Gu, Z.Y, Wu, N.Q., Xu B., 2007. Diet control on carbon isotopic composition of land  
664 snail shell carbonate. *Chin. Sc. Bull.* 52, 388-394.

665

666 Longinelli, A., Selmo, E., 2003. Isotopic composition of precipitation in Italy: a first overall map. *J.*

667 *Hydrol.* 270, 75–88.

668

669 López-Moreno, J.I., Vicente-Serrano, S.M., Morán-Tejeda, E., Lorenzo-Lacruz, J., Kenawya, A.,  
670 Benistonb, M., 2011. Effects of the North Atlantic Oscillation (NAO) on combined temperature and  
671 precipitation winter modes in the Mediterranean mountains: Observed relationships and projections  
672 for the 21st century. *Glob. Planet. Ch.* 77, 62–76.

673

674 Ložek, V., 1990. Molluscs in loess, their paleoecological significance and role in geochronology  
675 principals and methods. *Quat. Int.* 7/8, 71-79.

676

677 Marcolini, F., Bigazzi, G., Bonadonna, F.P., Centamore, E., Cioni, R., Zanchetta, G., 2003.  
678 Tephrochronology and tephrostratigraphy of two Pleistocene continental fossiliferous successions  
679 from Central Italy. *J. Quat. Sc.*, 18, 545-556.

680

681 Marra, F., Karner, D.B., Freda, C., Gaeta, M., Renne, P. 2009. Large mafic eruptions at Alban Hills  
682 Volcanic District (Central Italy): Chronostratigraphy, petrography and eruptive behavior. *J.*  
683 *Volcanol. Geoth. Res.* 179, 217–232.

684

685 Metref, S., Rousseau, D.-D., Bentaleb, I., Labonne, M., Vianey-Liaud, M., 2003. Study of the diet  
686 effect on  $\delta^{13}\text{C}$  of shell carbonate of the land snail *Helix aspersa* in experimental conditions. *Earth*  
687 *Planet. Sc. Lett.* 211, 381-393.

688

689 Mix, A.C., Ruddiman, W.F., 1984. Oxygen-Isotope Analyses and Pleistocene Ice Volumes. *Quat.*  
690 *Res.*, 21 1-20.

691

692 Moine, O., 2008. West-European Malacofauna from loess deposits of the Weichselian upper  
693 Pleniglacial: compilation and preliminary analysis of the database. *Quaternaire*, 19, 11-29.

694

695 Murelaga, X., Ortega, L.A., Sancho, C., Muñoz, A., Osácar, C., Larraz, M. 2012. Succession and  
696 stable isotope composition of gastropods in Holocene semi-arid alluvial sequences (Bardenas  
697 Reales, Ebro Basin, NE Spain): Palaeoenvironmental implications. *The Holocene* 22, 1047–1060.

698

699 Negri, A., Amorosi, A., Antonioli, F., Bertini, A., Florindo, F., Lurcock, P.C., Marabini, S.,  
700 Mastronuzzi, G., Regattieri, E., Rossi, V., Scarponi, S., Taviani, M., Zanchetta, G., Vai, G.B. 2015.  
701 A potential Global Stratotype Section and Point (GSSP) for the Tarentian Stage, Upper Pleistocene,  
702 from the Taranto area (Italy): Results and future perspectives. *Quat. Inter.*, 383, 145-157.

703

704 Patacca, E, Scandone, P. 2007. Geology of the Southern Apennines. *Boll. Soc. Geol. It.* 7, 75–

705 119.Patterson, W.P., Smith, G.R., Lohmann, K.C., 1993. Continental paleothermometry and  
706 seasonality using the isotopic composition of aragonitic otoliths of freshwater fishes. In: Swart,  
707 P.K., Lohmann, K.C., McKenzie, J., Savin, S. (Eds.), *Climate Change in Continental Isotopic*  
708 *Records: Geophys. Monogr. Ser.*, 78, 191–202.

709

710 Paul D., Mauldin R., 2013. Implications for Late Holocene climate from stable carbon and oxygen  
711 isotopic variability in soil and land snail shells from archaeological site 41KM69 in Texas, USA.  
712 *Quat. Int.*, 308-309, 242-252.

713

714 Pyankov, V., Ziegler, H., Akhiani, H., Deigele, C., Lüttge, U. 2010. European plants with C<sub>4</sub>  
715 photosynthesis: geographical and taxonomic distribution and relations to climate parameters.  
716 *Botanical Journal* 163, 283–304.

717

718 Prendergast, A.L., Stevens, R.E., Barker, G., O'Connell, T.C., 2015. Oxygen isotope signatures  
719 from land snail (*Helix melanostoma*) shells and body fluid: Proxies for reconstructing  
720 Mediterranean and North African rainfall. *Chem. Geol.* 409, 87–98.

721

722 Prendergast, A.L., Stevens, R.E., O'Connell, T.C., Hill, E.A., Hunt, C.O., Barker G.W. 2016. A late  
723 Pleistocene refugium in Mediterranean North Africa? Palaeoenvironmental reconstruction from  
724 stable isotope analyses of land snail shells (Haua Fteah, Libya). *Quat. Sc. Rev.*, 139, 94-19.

725

726 Prendergast, A.L., Stevens, R.E., Hill, E.A., Hunt, C., O'Connell, T.C., Barker, G.W. 2017. Carbon  
727 isotope signatures from land snail shells: Implications for palaeovegetation reconstruction in the  
728 eastern Mediterranean. *Quat. Int.* 432, 48-57.

729

730 Railsback, R.B., Gibbard, P.L., Head, M.J., Voarintsoa, N.R.G., Toucanne, S. 2015. An optimized  
731 scheme of lettered marine isotope substages for the last 1.0 million years, and the  
732 climatostratigraphic nature of isotope stages and substages, *Quat. Sci. Rev.*, 111, 94–106,

733

734 Razkin, O., Gómez-Moliner, B.J., Prieto, C.E., Martínez-Ortí, A., Arrébola, J.R., Muñoz, B.  
735 Chueca, L.J., Madeira, M.J., 2015. Molecular phylogeny of the western Palaeartic Helicoidea  
736 (Gastropoda, Stylommatophora). *Molecul. Phylogenet. Evol.*, 83, 99-117.

737

738 Regattieri, E., Zanchetta, G., Drysdale, R.N., Isola, I., Hellstrom, J.C., Roncioni, A., 2014. A

739 continuous stable isotopic record from the Penultimate glacial maximum to the Last Interglacial  
740 (160 to 121 ka) from Tana Che Urla Cave (Apuan Alps, central Italy). *Quat. Res.*, 82, 450–461.  
741

742 Regattieri, E., Giaccio, B., Zanchetta, G., Drysdale, R.N., Galli, P., Nomade, S., Peronace, E., Wulf,  
743 S. 2015. Hydrological variability over Apennine during the Early Last Glacial precession  
744 minimum, as revealed by a stable isotope record from Sulmona basin, central Italy. *J. Quat. Sc.*, 30,  
745 19-31.

746

747 Regattieri, E., Giaccio, B., Galli, P., Nomade, S., Peronace, E., Messina, P., Sposato, A., Boschi, C.,  
748 Gemelli, M. 2016. A multi-proxy record of MIS 11-12 deglaciation and glacial MIS 12 instability  
749 from the Sulmona basin (central Italy). *Quat. Sc. Rev.* 132, 129-145.

750

751 Regattieri, E., Giaccio, B., Nomade, S., Francke, A., Vogel, H., Drysdale, R.N., Perchiazzi, N.,  
752 Wagner, B., Gemelli, M., Mazzini, I., Boschi, C., Galli, P., Peronace E., 2017. A Last Interglacial  
753 record of environmental changes from the Sulmona Basin (central Italy). *Palaeogeogr.*,  
754 *Palaeoclimatol.*, *Palaeoecol.* 472, 51–66.

755

756 Retallack, G.J. 2005. Pedogenic carbonate proxies for amount and seasonality of precipitation in  
757 paleosols. *Geology*, 33, 333-336.

758

759 Roberts, N., Jones, M.D., Benkaddur, A., Eastwood, W.J., Filippi, M.L., Frogley, M.R., Lamb,  
760 H.F., Leng, M.J., Reed, J.M., Stein, M., Stevens, L., Valero- Garcè, B., Zanchetta, G., 2008 Stable  
761 isotope records of Late Quaternary climate and hydrology from Mediterranean lakes: the ISOMED  
762 synthesis. *Quat. Sc. Rev.*, 27, 2426-2441.

763

764 Romanek, C.S., Grossman, E.L., Morse, J.W., 1992. Carbon isotopic fractionation in synthetic  
765 aragonite and calcite: effects of temperature and precipitation rate. *Geochim. Cosmochim. Acta* 56,  
766 419–430.

767

768 Romaniello, L., Quarta, G., Mastronuzzi, G., d'Elia, M., Calcagnile, L., 2008. <sup>14</sup>C age anomalies in  
769 modern land snails shell carbonate from Southern Italy. *Quat. Geochronol.* 3, 68-75.

770

771 Rousseau, D.-D., Puisségur, J.J., Lautridou, J.P., 1990. Biogeography of the Pleistocene

772 Pleniglacial malacofaunas in Europe. *Palaeogeogr., Palaeoclimatol., Palaeoecol.* 80, 7–23.  
773

774 Rousseau, D.-D., Puisségur, J.J., Lécalle F., 1992. Mollusc assemblages of isotopic stage 11  
775 (Middle Pleistocene): climatic implications. *Palaeogeogr., Palaeoclimatol., Palaeoecol.*, 92: 15–29.  
776

777 Rozanski, K., Araguás-Araguás, L., Gonfiantini, R., 1993. Isotopic patterns in modern global  
778 precipitation, in: P.K. Swart, K.C. Lohmann, J. McKenzie, S. Savin (Eds.), *Climate Change in*  
779 *Continental Climate Records*, Am. Geophys. Union, *Geophys. Monogr.* 78, 1–36.  
780

781 Sacchi, C.F., 1952. Raggruppamenti di molluschi terrestri sul litorale Italiano. Considerazioni e  
782 ricerche introduttive. *Bollettino della Società Veneziana di Storia Naturale e del Museo Civico di*  
783 *Storia Naturale*, 6: 99-158.  
784

785 Sagnotti, L, Scardia, G, Giaccio, B., et al. 2014. Extremely rapid directional change during  
786 Matuyama-Brunhes geomagnetic polarity reversal. *Geophys. J. Int.* 199, 1110–1124.  
787

788 Sarti, G., Zanchetta, G., Ciulli, L., Colonese, A., 2005. Late Quaternary oligotypical non-marine  
789 mollusc fauna from southern Tuscany: climatic and stratigraphic implications. *Geoacta*, 4, 159-167.  
790

791 Sparks, B.W., 1961. The ecological interpretation of Quaternary non-marine Mollusca. *Proc. Linn.*  
792 *Soc. Lond.* 172, 71-80.  
793

794 Stott, L.D., 2002. The influence of diet on the  $\delta^{13}\text{C}$  of shell carbon in the pulmonate snail *Helix*  
795 *aspersa*. *Earth Planet. Sc. Lett.* 195, 249-259.  
796

797 Tarutani, T., Clayton, R.N., Mayeda, T.K., 1969. The effect of polymorphism and magnesium  
798 substitution on oxygen isotope fractionation between calcium carbonate and water. *Geochim.*  
799 *Cosmochim. Acta* 33, 987–996.  
800

801 Tzedakis, P. C., Hooghiemstra, H., and Pälike, H. 2006. The last 1.35 million years at Tenaghi  
802 Philippon: revised chronostratigraphy and long-term vegetation trends, *Quat. Sci. Rev.*, 25, 3416–  
803 3430.  
804

805 Wang, Y, Zheng, S. 1989. Paleosol nodules as Pleistocene paleoclimatic indicators, Louchuan, P.R.  
806 China. *Palaeogeogr., Palaeoclimatol., Palaeoecol.*, 76, 39–44.



807

808 Welter-Schultes F., 2012. European non-marine molluscs, a guide for species identification.  
809 Bestimmungsbuch für europäische Land- und Süßwassermollusken. Planet Poster Editions.  
810 Göttingen: 1-679, quick identification plates: Q1-Q78.

811

812 Yanes, Y., Delgado, A., Castillo, C., Alonso, M.R., Ibáñez, M., De la Nuez, J., Kowalewski, M.,  
813 2008. Stable isotope ( $\delta^{18}\text{O}$ ,  $\delta^{13}\text{C}$ , and  $\delta\text{D}$ ) signatures of recent terrestrial communities from a low-  
814 latitude, oceanic setting: endemic land snails, plants, rain, and carbonate sediments from the eastern  
815 Canary Islands. *Chem. Geol.* 249, 277-292.

816

817 Yanes, Y., Romanek, C.S., Delgado, A., Brant, H.A., Noakes, J.E., Alonso, M.R., Ibáñez, M., 2009.  
818 Oxygen and carbon stable isotopes of modern land snail shells as environmental indicators from a  
819 low-latitude oceanic island. *Geochim. Cosmochim. Acta* 73, 4077-4099.

820

821 Yanes, Y., Romanek, C.S., Molina, F., Cámara, J., Delgado, A., 2011. Holocene paleoenvironment  
822 (7200–4000 cal BP) of the Los Castillejos archaeological site (SE Spain) inferred from the stable  
823 isotopes of land snail shells. *Quat. Inter.* 244, 67–75.

824

825 Yates, T.J.S., Spiro, B.F., Vita-Finzi, C., 2002. Stable isotope variability and the selection of  
826 terrestrial mollusc shell samples for  $^{14}\text{C}$  dating. *Quat. Int.* 87, 87-100.

827

828 Villa, V., Pereira, A., Chauss, C., Nomade, S., Giaccio, B., Lomondin-Lozouet, N., Fusco, F.,  
829 Regattieri, E., Degeai, J.-P., Robert, V., Kuzucuoglu, C., Boschian, G., Agostini, S., Aureli, D.,  
830 Pagli, M. Bahain, J.J., Nicoud, E. 2016. A MIS 15-MIS 12 record of environmental changes and  
831 Lower Palaeolithic occupation from Valle Giumentina, central Italy. *Quat. Sc. Rev.* 151, 160-184.

832

833 Zanchetta, G., Bonadonna, F.P., Leone, G., 1999. A 37-meter record of paleoclimatological  
834 events from stable isotope data on molluscs in Valle di Castiglione, near Rome, Italy. *Quat.*  
835 *Res.*, 52, 293-299.

836

837 Zanchetta, G., Bonadonna, F.P., Ciampalini, A., Colonesi, A., Dall'Antonia, B., Bossio, A., Fallick,  
838 A.E., Leone, G., Marcolini, F., Michelucci, L., 2006. Late Middle Pleistocene cool non-marine  
839 mollusc and micromammal faunas from Livorno (Italy). *Riv. It. Paleontol. Strat.*, 112, 135-155.

840

841 Zanchetta, G., Borghini, A., Fallick, A.E., Bonadonna, F.P., Leone, G. 2007a. Late Quaternary  
842 palaeohydrology of Lake Pergusa (Sicily, southern Italy) as inferred by stable isotopes of lacustrine  
843 carbonates. *J. Paleolimnol.*, 38, 227-239.

844

845 Zanchetta, G., Drysdale, R.N., Hellstrom, J.C., Fallick, A.E., Isola, I., Gagan, M., Pareschi, M.T.  
846 2007b. Enhanced rainfall in the western Mediterranean during deposition of Sapropel S1: stalagmite  
847 evidence from Corchia Cave (Central Italy). *Quat. Sc. Rev.*, 26, 279-286.

848

849 Zanchetta, G., Di Vito, A., Fallick, A.E., Sulpizio, R., 2000. Stable isotopes of pedogenic  
850 carbonate from Somma-Vesuvius area, Southern Italy, over the last 18 ka: palaeoclimatic  
851 implications. *J. Quat. Sc.*, 15, 813-824.

852

853 Zanchetta, G., Leone, G., Fallick, A.E., Bonadonna, F.P. 2005. Oxygen isotope composition of  
854 living land snail shells: data from Italy. *Palaeogeogr., Palaeoclimatol., Palaeoecol.*, 223, 20-33.

855

856 Zanchetta, G., Regattieri, E., Isola, I., Drysdale, R.N, Bini, M., Baneschi, I., Hellstrom, J.C., 2016.  
857 The so-called “4.2 event” in the central Mediterranean and its climatic teleconnections. *Alpine and*  
858 *Mediterranean Quaternary*, 29, 5 – 17.

859

## Figure and table captions

Figure 1. Location map, geological sketch map and general stratigraphy of the area. SC1 hole is discussed in Sagnotti et al., 2014 and Regattieri et al., 2015.

Figure 2. General stratigraphy of the lacustrine succession of the Sulmona Basin, with details of Fiorata paleosol succession and age constraints for the formation of the soil. Main tephra layers are indicated along with  $^{40}\text{Ar}/^{39}\text{Ar}$  dating. The isotopic curve is from Lisičky and Raymo (2005). Tephrostratigraphy and  $^{40}\text{Ar}/^{39}\text{Ar}$  dating from Giaccio et al. (2012; 2013a; 2013b; 2015); Sagnotti et al. (2014); Regattieri et al. (2015; 2016; 2017).

Figure 3. The most represented land snail species in Fiorata paleosol: *Pupilla muscorum* (top), *Vallonia costata* (middle) and an unidentified geometrid helicelline (bottom).

Figure 4. Example of X-ray powder diffraction patterns of the small pedogenic concretions (a) and terrestrial shells (b). Main diffraction lines are shown ( $d_{hkl}$  in Å). In (a), colors refer to diffraction lines of different minerals: blue = calcite; red = quartz; yellow = mica; and green = feldspar. In (b), all the diffraction lines belong to aragonite; (c) details of pedogenic concretions, showing typical shape of hypocoating.

Figure 5. Carbon and oxygen isotopic data from lacustrine deposits of Sulmona Basin (Regattieri et al., 2016), shell and pedogenic carbonate from Fiorata paleosol (this work); and clastic carbonate (Villa et al. 2016; Regattieri et al., 2016). VG: Valle Giumentina.

Table 1. Landsnails species and their ecological requirement.

Table 2. Stable isotope composition of land snail shells and pedogenic carbonate from the Fiorata Paleosol.

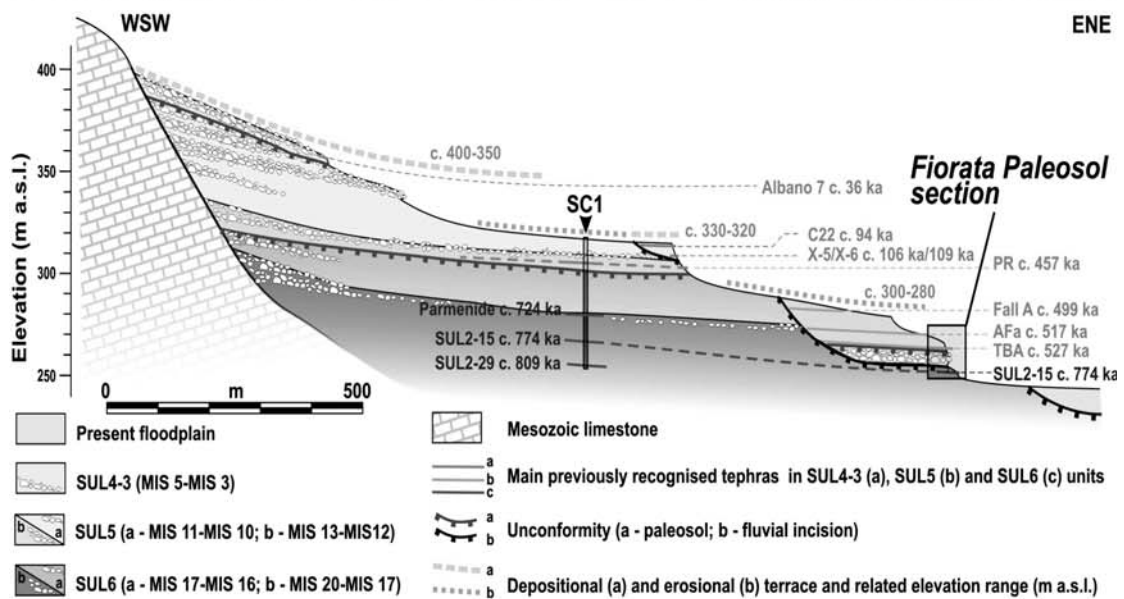
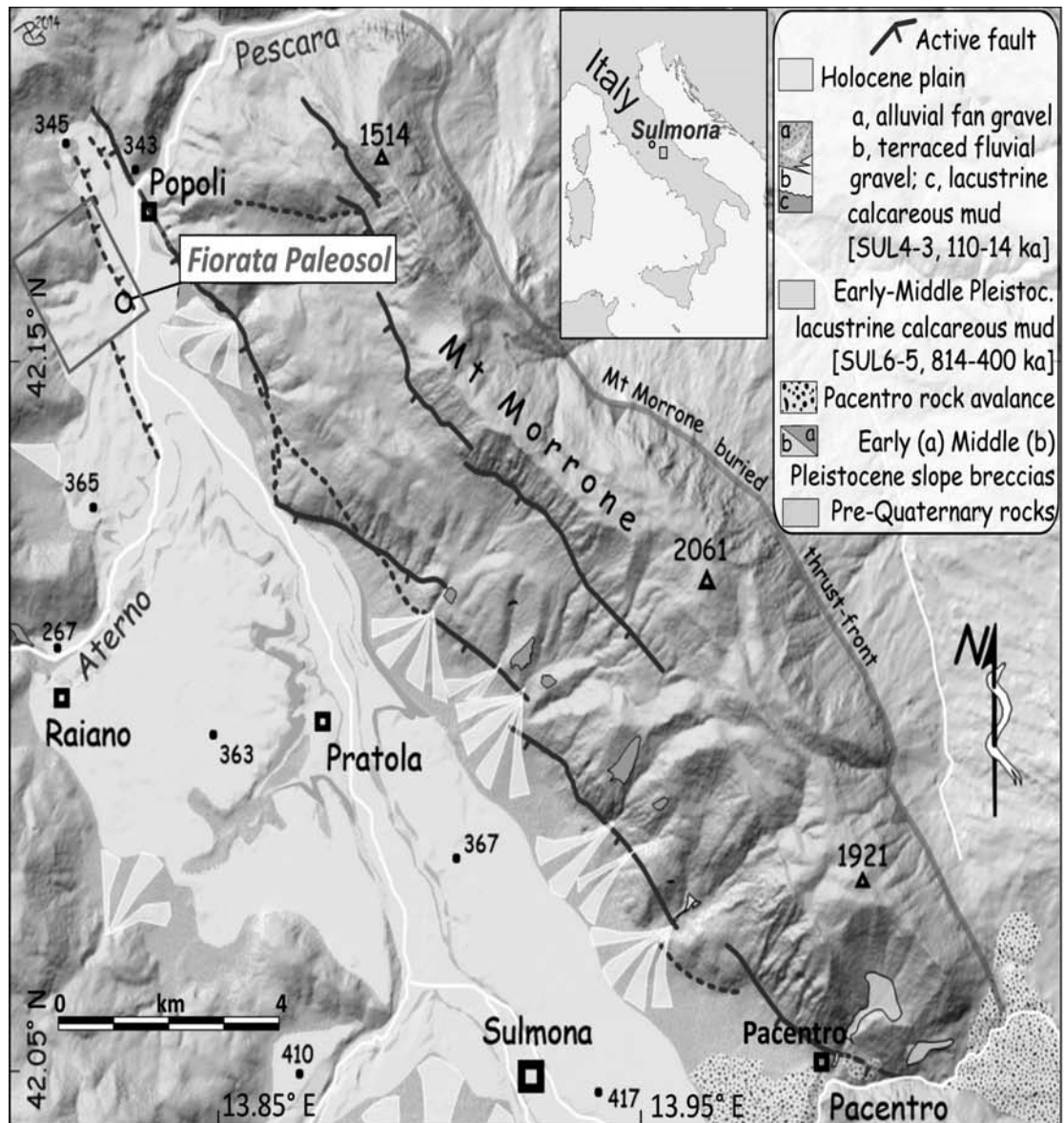
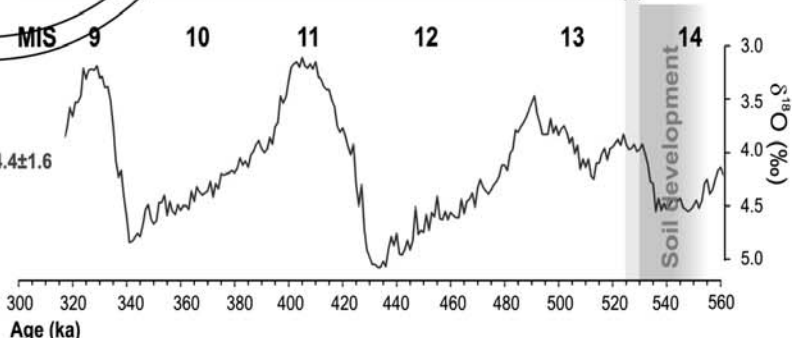
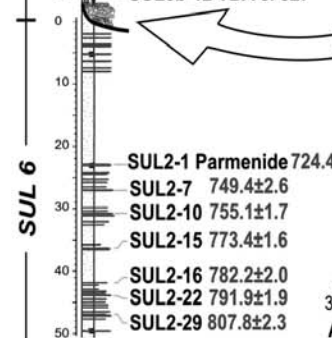
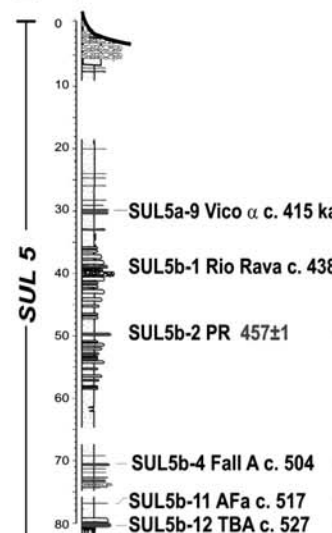
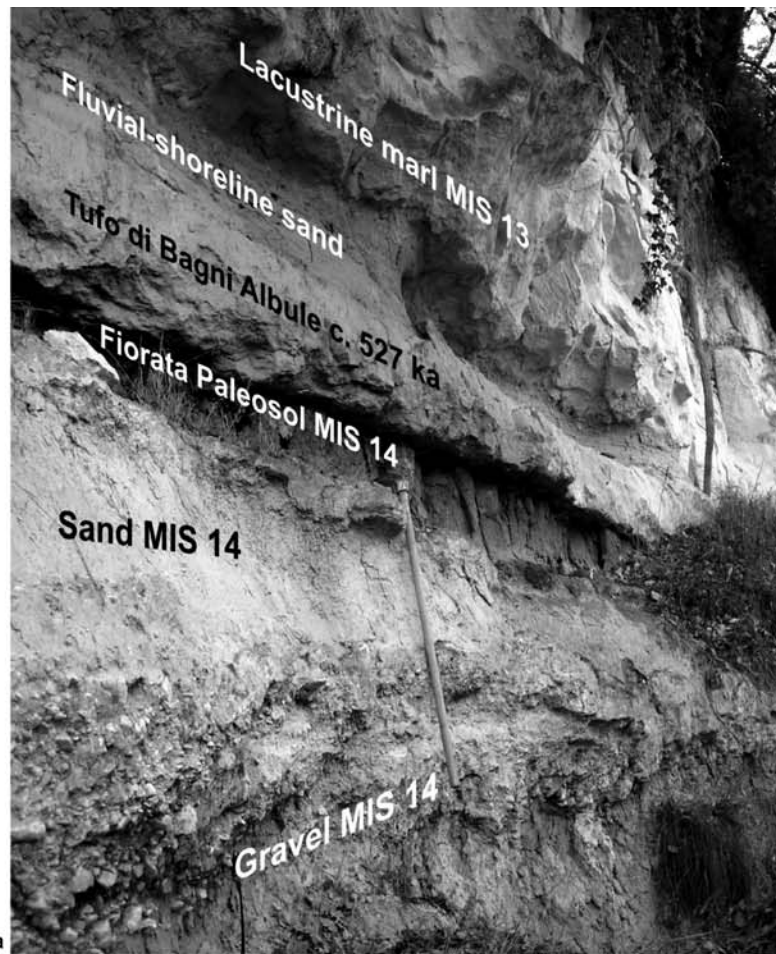
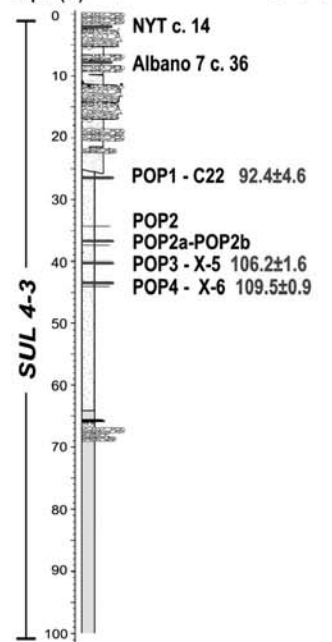


Fig.1

### Sulmona composite section

Depth (m) Tephra and related age (ka)



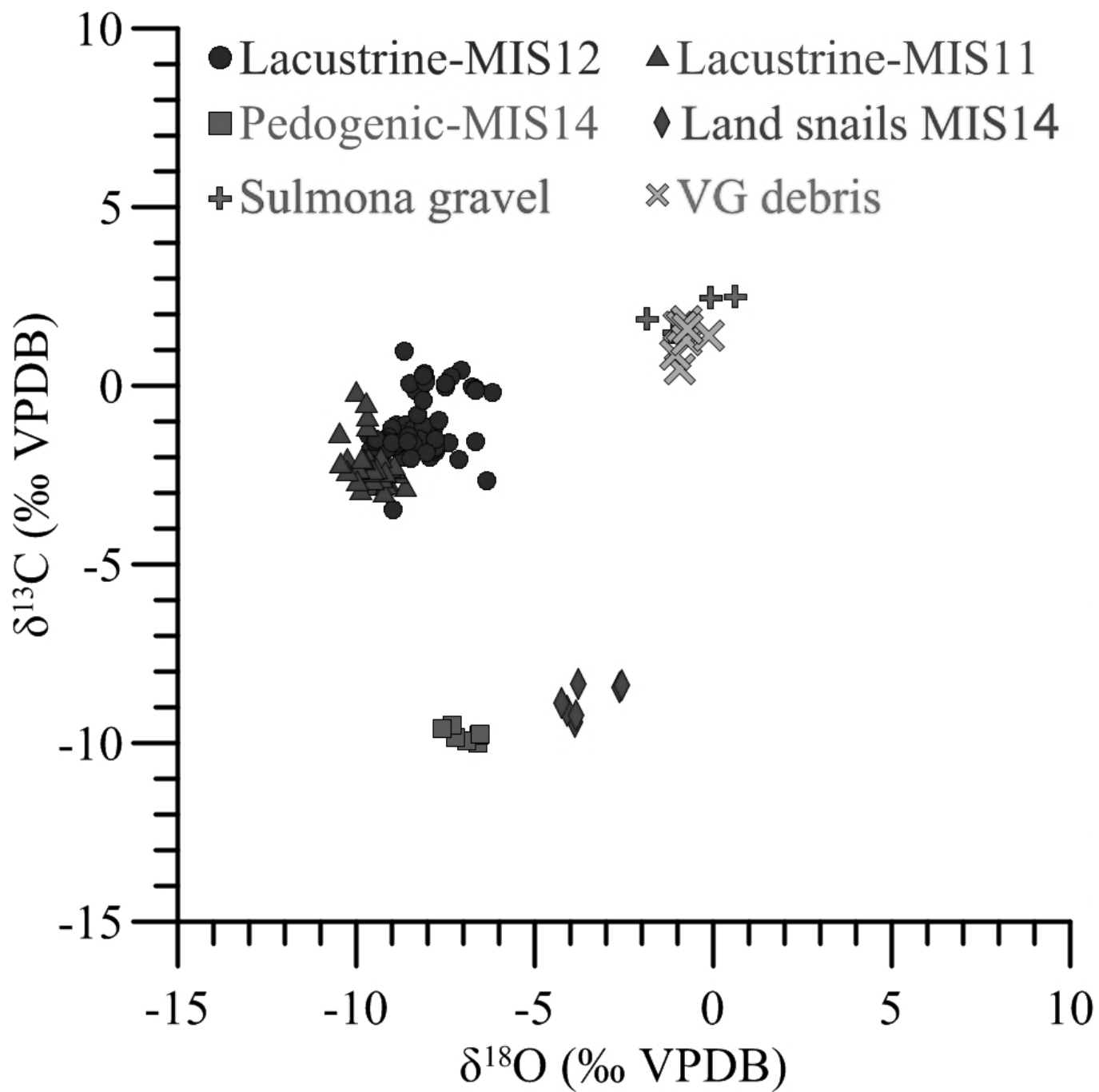
- |  |                                    |  |                         |  |              |
|--|------------------------------------|--|-------------------------|--|--------------|
|  | Lacustrine whitish marls           |  | Fluvial/lacustrine sand |  | Paleosol     |
|  | Lacustrine-palustrine greyish clay |  | Fluvial/alluvial gravel |  | Tephra layer |
|  | Peat                               |  |                         |  |              |
- 106.2±1.6 <sup>40</sup>Ar/<sup>39</sup>Ar age (ka) of Sulmona tephra  
 c. 36 <sup>40</sup>Ar/<sup>39</sup>Ar age (ka) of correlated tephra

Fig.2









Species and higher systematics	Material	Main habitats
<b>Caenogastropoda, Hypsogastropoda, Pomatiidae</b>		
<i>Pomatias elegans</i> (Müller, 1774)	2 sps: one operculum of a juvenile and one last whorl fragment of an adult/subadult	dry to mesophilous woodland edges and glades
<b>Heterobranchia, Pulmonata, Orthurethra, Vertiginidae</b>		
<i>Truncatellina cylindrica</i> (Férussac, 1807)	2 sps: two incomplete shells	mesophilous open habitats
<b>Heterobranchia, Pulmonata, Orthurethra, Pupillidae</b>		
<i>Pupilla muscorum</i> (Linnaeus, 1758)	> 16 sps: many well preserved shells	dry to mesophilous open habitats
<b>Heterobranchia, Pulmonata, Orthurethra, Valloniidae</b>		
<i>Vallonia costata</i> (Müller, 1774)	32 sps many badly preserved shells	mesophilous open habitats and woodlands
<b>Heterobranchia, Pulmonata, Orthurethra, Enidae</b>		
<i>Jaminia</i> sp.	2 sps: two shell apices	dry open habitats
<b>Heterobranchia, Pulmonata, Sigmurethra, Geomitridae, Helicellinae</b>		
Unidentified helicelline geomitrid	> 70 sps: many fragmentary shells	dry open habitats

Table 1. Landsnails species and their ecological requirement.

Sample label	$\delta^{13}\text{C}$ ‰ (V-PDB)	$\delta^{18}\text{O}$ ‰ (V-PDB)
Pedogenic carbonate		
SUL14-1	-10.02	-6.58
SUL14-2	-9.80	-6.57
SUL14-3	-9.95	-6.90
SUL14-4	-9.52	-7.22
SUL14-14a	-9.52	-7.31
SUL14-12	-9.77	-6.54
SUL14-13	-9.60	-7.60
<b><i>Average (<math>\pm 1</math> st dev)</i></b>	<b><i>-9.79 <math>\pm</math> 0.18</i></b>	<b><i>-6.96 <math>\pm</math> 0.42</i></b>
<i>Land snail shell</i>		
SUL14-6	-9.42	-3.88
SUL14-7	-9.11	-4.10
SUL14-8	-8.45	-2.63
SUL14-9	-8.34	-3.77
SUL14-10	-8.89	-4.26
SUL14-11	-9.23	-3.85
SUL14-11a	-8.39	-2.55
<b><i>Average (<math>\pm 1</math> st dev)</i></b>	<b><i>-8.83 <math>\pm</math> 0.44</i></b>	<b><i>-3.10 <math>\pm</math> 0.69</i></b>

Table 2 Stable isotope composition of land snail shells and pedogenic carbonate from the Fiorata paleosol

## Highlights

Mollusks association from Fiorata Paleosol indicates dry climate during late MIS14.

Carbon isotopes of pedogenic carbonates and land shells support the notion of dry climate.

Oxygen isotope composition of pedogenic carbonate and shells suggest lower 3-5 °C temperature than present.